Design, Fabrication, and *In Vitro* Evaluation of an *In Vivo* Ultrasonic Doppler Wall Shear Rate Measuring Device

Robert S. Keynton, Richard E. Nemer, Qianhui Y. Neifert, Ray S. Fatemi, and Stanley E. Rittgers

***Abstract*—*In vivo* wall shear rates have been obtained based on estimates from either volume flow rate or single-point velocity measurements along with the wall no slip assumption and a simple linear regression. Recent results [19] have shown that, under pulsatile flow conditions, wall shear rates are more accurately predicted by using up to four velocity points and a second- or third-order polynomial curve fit. It is the purpose of this paper to evaluate the accuracy of a new, *in vivo* transducer capable of determining wall shear rates nonintrusively from velocities at three points along a line perpendicular to the vessel wall. Three 20-MHz ultrasound crystals were imbedded in an elastomer at distances of 1.5 and 2.1 mm with beam angles of 30°, 45°, and 60° to the horizontal plane. Microscopic examination showed that intercrystal spacings were within 1.5% of the design and the crystal angles were placed within 2.0%. *In vitro* calibration was performed under steady and pulsatile flow conditions with average shear rates being within 4.3 ± 17.3% and 0.2 ± 0.6%, respectively, of the theoretically predicted values. Furthermore, peak and oscillatory shear rates were within −5.6 ± 2.2% and −2.4 ± 5.7% accuracy, respectively. Results from this study show this device to be capable of providing accurate wall shear rates *in vivo*.**

I. Introduction

HEMODYNAMICS in general and wall shear in particular have been widely associated with development of atherosclerosis [1]–[5] and intimal hyperplasia [6]–[11]. Electrochemical techniques have been applied in studies using *in vitro* models to make direct shear measurements [12], [13]. While these devices are capable of being highly accurate, they suffer from invasiveness, insensibility to direction and pulsatility of flow, and fixed measurement locations. Consequently, most reports of shear measurements have employed a more versatile, although less direct, approach based on the detection of flow velocities near the vessel wall and with shear rate determined as the velocity slope at the wall.

Studies of complex *in vivo* geometries have generally employed either qualitative [4] or simplified indirect [2], [14]–[16] techniques to determine shear rate. More exact measurements have been obtained using hot-film anemometry (HFA) [6] and ultrasound pulse Doppler (PUDV) [17], [18] velocity recordings to compute shear. From recent work carried out in the laboratory [19], it has been shown that shear rate measurements can be made under pulsatile conditions to within ± 20% accuracy using four velocity points (three free stream measurements together with the wall no-slip condition) and either a second- or third-order polynomial curve fit. While these results were based on laser Doppler anemometry (LDA) measurements from an *in vitro* model at radial intervals of 100 μm (= 0.04 diameters), it is felt that application of the same procedure to ultrasonic pulse Doppler velocities measured using small radial intervals would provide adequate results under *in vivo* conditions.

Previously reported single or multigate ultrasound pulse Doppler devices [20], [21] were limited to velocity measurements made along the ultrasound beam at an angle to the flow and were, thus, unable to obtain true cross-sectional velocity slopes (i.e., shear rates) at a given axial location. Therefore, it is the purpose of this paper to introduce and validate an ultrasound transducer capable of nonintrusively obtaining vascular wall shear rates *in vivo* within medium to large size arteries.

Manuscript received April 27, 1994; revised December 14, 1994. This work was supported by the National Institute on Aging/NIH Grant 1 R03 AG10398-01, NIH/NCRR Grant 1 F31 RR05054-01, W. L. Gore and Associates, the Ohio Board of Regents Academic Challenge Program, and the Summa Health System Foundation.

R. S. Keynton, R. E. Nemer, Q. Y. Neifert, and R. S. Fatemi are with the Department of Biomedical Engineering, University of Akron, Akron, OH 44325-0302 USA.

S. E. Rittgers is with the Department of Biomedical Engineering, University of Akron, Akron, OH 44325-0302 USA and the Vascular Hemodynamics Research Laboratory, Summa Health System, Akron, OH 44309 USA.

IEEE Log Number 9410037.

II. Materials and Methods

A. Instrument Design Criteria

In order to satisfy the requirements of nonintrusiveness, high resolution, and the ability to operate under *in vivo* conditions, a shear rate transducer was designed based on high frequency pulse ultrasonic Doppler velocity (PUDV) detection at multiple points along the vessel radius. Specifically, a 20-MHz pulse Doppler system was chosen due to its small sample volume (0.31 mm × 0.785 mm^2) and its sufficient depth of penetration (10 mm). One disadvantage of a high-frequency device is the greater risk of velocity aliasing, but since this system is intended for use with unstenosed vessels, it was felt that the extreme axial velocities which would produce aliasing (> 142 cm/s based on a 30° beam to flow angle) were unlikely to be encountered.

A transducer configuration was developed utilizing three 20-MHz ultrasound crystals (d = 1 mm) placed along a straight line with beam angles of 30°, 45°, and 60° to the plane of flow at corresponding interval spacings of 1.5 mm and 2.1 mm (Fig. 1). This configuration, together with a sampling length of 0.31 mm (4–6λ) and proper choice of individual range distances, enables measurement of velocity components

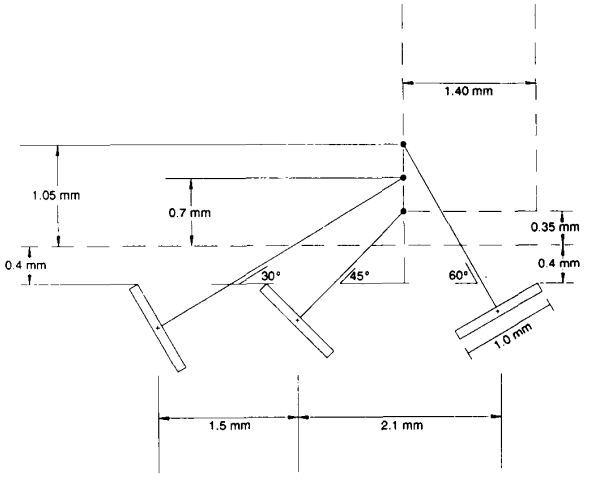

Fig. 1. Schematic of triple crystal, 20-MHz shear rate transducer.

at *radial* positions of 0.35 mm, 0.7 mm, and 1.05 mm from the vessel wall (assumed to be 0.4 mm thick [22]) at any axial position. All the measuring points are within the near fields of the transducers since a 1-mm wide ultrasound crystal operating at a frequency of 20 MHz has a near field of 3.33 mm. In addition to the above-mentioned criteria, this design also minimized the distance between the line of velocity measurement (perpendicular to the face of the transducer) and the end of the transducer—a feature necessary in order to make shear rate measurements close to structures such as the anastomotic toe of a bypass graft and artery. This design represents a modification from an earlier one which did not account for vessel wall thickness [23].

B. Fabrication of Transducer

Each shear rate transducer was fabricated using a jig containing positioning rods to precisely locate the individual ultrasound crystals within a silastic matrix. The rods were formed from 18-gauge needles (Becton Dickinson, Rutherford, NJ) machined to yield tip angles of 30°, 45°, and 60° from the cross-sectional plane of the needles. These angles were measured using a shadow comparator (EPIC 114, Jones and Lamson, York, SC) and found to be 30.5°, 44.7°, and 58°, respectively. A rectangular recession was machined into an aluminum block and three holes were drilled with 1.5 mm and 2.1 mm spacings between centers along the mid-line of the block. The needles were then silver-soldered into the drilled holes. The center of an aluminum jig cap was machined with a recessed hole to form a mold around the positioning rods. Threaded holes on either side of the jig cap allowed for screws which were used to lift the molded transducer from the jig following completion of the silastic curing process.

The 20-MHz PZT-5A crystals (DBF-120A-XS, Crystal Biotech, Hopkinton, MA) were preassembled by silver-soldering color-coded 34-gauge, silver-plated copper wire leads to the piezoelectric material. The wire leads were passed through the center of each needle and the crystals were carefully placed on the tips of the needles and aligned so that the exposed edges of the crystals were flush mounted to an imaginary horizontal line. The mold and needles were coated with a releasing agent, the jig cap was placed over the needles, and silastic (Sylgard/Silastic 732, Dow Corning, Midland, MI) was poured into the mold and cured at 60°C for 4–6 h. The molded piece was removed and the holes left by the needles were then back filled with silastic and allowed to cure for an additional 4–6 h. This procedure was comparable to fabrication techniques which used a styrofoam backing, both of which produced between 4.5–6 cycles per pulse burst and satisfied the requirements needed for Doppler-shift frequency processing.

Excess silastic was cleared from the top surface of the crystals and an epoxy coating was then applied to the wire lead exiting from the exposed face of the crystal to prevent corrosion of the wire leads. The wire leads were covered with heat shrink tubing (Heatrax, Ico-Rally Corp., Palo Alto, CA) and the ends were silver-soldered to modified machine pin sockets to provide a protected electrical connection to the ultrasound Doppler demodulators.

C. Instrumentation

The ultrasound crystals were interfaced with commercially available Doppler instrumentation (Model VF-1, Crystal Biotech, Hopkinton, MA) which included a master oscillator (Doppler Master, Model DM-1, Crystal Biotech, Hopkinton, MA) and directional demodulator (Model PD-20, Crystal Biotech, Hopkinton, MA). The crystals were each driven by a 20-MHz transmitting signal at a nominal pulse repetition frequency (PRF) of 62.5 kHz which generated a gate size of 200 ns (0.31 mm). In order to operate the three crystals as a unit and avoid interference, the Doppler demodulators were modified to excite the downstream facing crystal (#1) 180° out of phase with the two upstream facing crystals (#2 and 3). This resulted in a 50% reduction in the PRF and also necessitated reducing the cut-off frequency of the low-pass filter from 50 kHz to 19 kHz. These modifications were adequate under *in vitro* conditions and preliminary investigations of flow in canine common carotid arteries (CCA) where the velocities and Doppler shift frequencies were low. However, in an end-to-side bypass graft configuration of the canine CCA, the Doppler shift frequencies were well above the cut-off frequency and aliasing was observed (note: *In vivo* application of this device is currently being conducted in our laboratory and will be presented in a subsequent paper). This led to a second modification (Fig. 2) where crystal #1 was alternately excited with crystals #2 and #3 using the ECG waveform as a trigger. This resulted in velocity data being collected on alternating cardiac cycles and thus required a doubling of the total record length.

The received ultrasound signals first underwent high-pass filtering (F_c = 160 Hz) followed by quadrature demodulation and zero-crossing counter (ZCC) detection on each directional channel. Since the ZCC detects the root mean square (rms) frequency of the signal being processed, it corresponds to the mean quadrature frequency only when the sample volume becomes infinitesimally small. Therefore, a pilot study using *in vivo* arterial recordings was conducted to determine the correlation between the rms and mean quadrature frequency

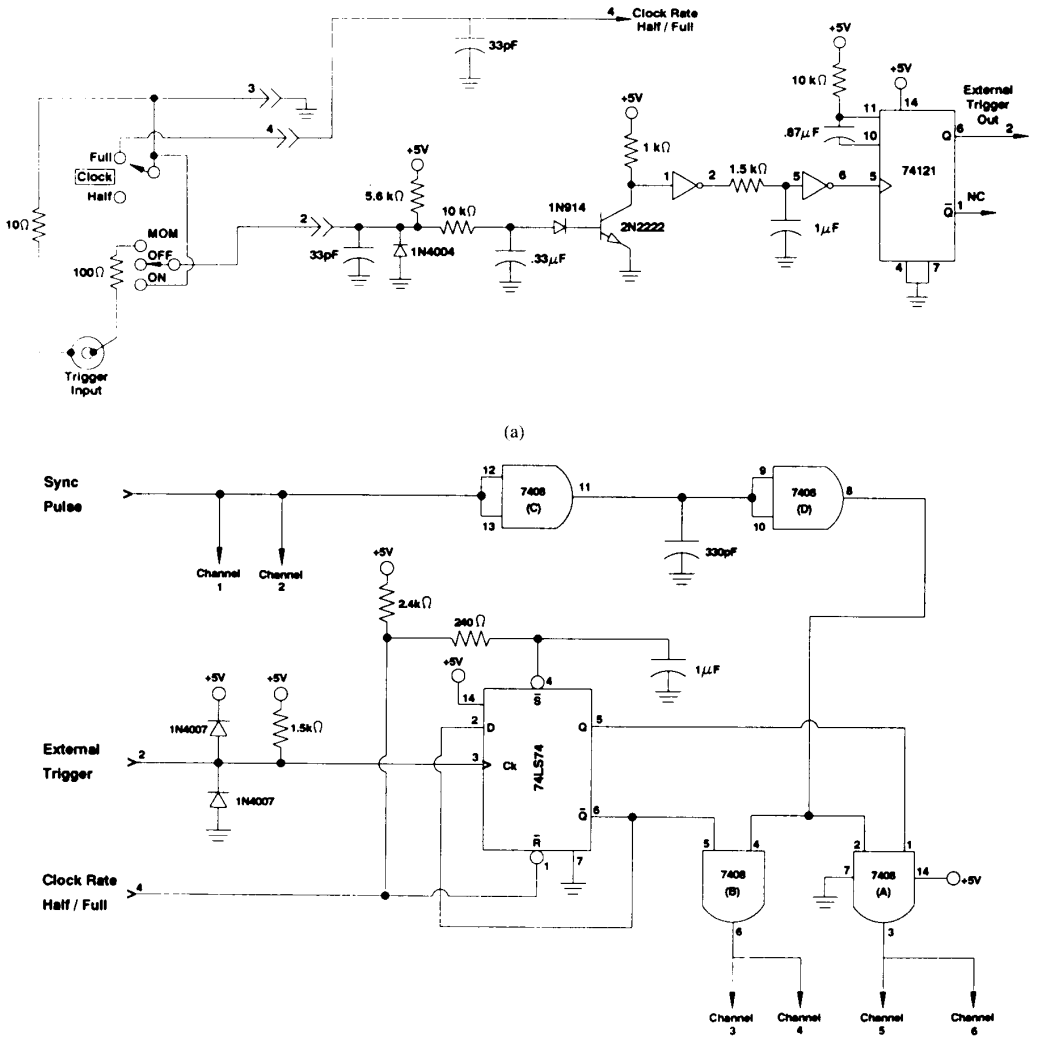

Fig. 2. Schematics of the modifications to the Doppler instrumentation. (a) ECG input signal conditioner. (b) Trigger enable multiplexer.

outputs using a computer simulation. The results showed that the two outputs were linearly related with the cross-correlation coefficients ranging from 0.990–1.000, thus justifying use of the rms output. The ZCC data was further compared to the corresponding output of a spectrum analyzer (Vasculab Model SP25A, MedaSonics, Mountain View, CA) and found to have a mean percent error of 3.1 ± 8.2% and no error greater than 17%. The range gate voltage output of each demodulator was calibrated against the range gate timing output and linear relationships were obtained for use in correcting the range settings. Furthermore, it was desired to have the center of the sample volume at the predetermined depth, and since the range output represents the distance to the tail of the sample volume, the sample volume range was shortened by 0.155 mm (1/2 the sample volume length).

An *in vitro* pilot study was performed to determine the number of cycle averages and sampling rate needed to accurately represent the data. A correlation study was conducted to determine the association between the ZCC output obtained with averages of 1, 4, 8, 12, and 16 waveforms, respectively, compared to that obtained with 32 waveforms. For each radial position (0.35 mm, 0.7 mm, and 1.05 mm), the cross-correlation coefficients for the 1, 4, 8, 12, and 16 averages were found to range from 0.998–1.000, 0.999–1.000, and 0.999–1.000, respectively. In addition, a backward elimination general linearized model regression was performed which indicated that no single waveform was significantly different ($p < 0.01$) from the other 31 waveforms. Thus, velocities obtained from an average of four cycles were not different from values obtained with an average of 32 cycles. Since collection of data over four cycles saves considerable time, disk space, and data processing, this procedure was selected. In order to determine the appropriate sampling rate, the directly accessible analog signal from the ZCC outputs of

all three crystals together with ECG timing information were simultaneously recorded on a four-channel digital oscilloscope (UnkelScope, Cambridge, MA) at a sampling rate of 2000 Hz, generating 4096 data points, which were averaged over four cycles and stored on disk. Subsequently, discrete Fourier transform analysis (Windaq, Dataq, Akron, OH), low-pass digital filtering (F_c = 50 Hz), and waveform reconstruction was performed on each velocity waveform. A Model I analysis of variance was performed between the respective velocity waveforms and found that the low-pass filtered waveforms were not significantly different ($p < 0.001$) from the unfiltered velocity waveforms. In addition, power spectral analysis was performed which showed that at least 94% of the velocity information was contained within the first 50 Hz of the signal. Therefore, a 100-Hz sampling rate generating 1024 data points was selected for this study. The A/D converter and digital oscilloscope were calibrated using the recorder calibrator on the VF-1 control box and a digital multimeter (Fluke 45, John Fluke Mfg. Co., Inc., Everett, WA). The output of the A/D converter-digital oscilloscope system was found to be nonlinearly related to the true voltage and a second-order regression equation was determined to correct measured values.

D. In Vitro Validation

After fabrication, the angles of the crystals were validated using a video light microscope with a 50× magnification lens (VH6100-VH50K, Keyence Corp., Newark, NJ). Validation of the velocity measured by the transducers was performed under both steady and pulsatile flow conditions using an interchangeable flow loop system. The system was instrumented with a differential pressure transducer (Model P305D-3-40-1100, Validyne, Northridge, CA) and an ultrasonic flowmeter and flow probe (T108 and 16NS-B-T208-CH10, Transonic Systems, Inc., Ithaca, NY). The flow loop was filled with a solution of 6.9 weight % Dextran ($2 \times 10^5 - 3 \times 10^5$ MW), 0.2 weight % cornstarch and distilled water which yielded a dynamic viscosity of 8.26 cP and a density of 1.02 g/cm^3. Since the ultrasonic flowmeter signal was sensitive to the concentration of cornstarch in solution, a time collection procedure was performed before and after each data collection to evaluate the effects of particle settling. Subsequently, a linear regression was performed on the time collection and flowmeter data to obtain a calibration curve for predicting the true flow values. The shear rate transducers were flush mounted to the inner wall of a 16-mm I.D. Plexiglas tube at 100 diameters from the inlet and were in direct contact with the fluid in order to reduce attenuation.

For steady flow, the submersible centrifugal pump was connected to the outflow tubing of the reserve tank and the left ventricular assist device (LVAD) was disabled. The system operated at a mean flow rate of 666 mL/min, corresponding to a mean Reynolds number of 110. Under these conditions, the tube length (L = 160 cm) was more than adequate to provide laminar fully developed flow. Laser Doppler anemometry (LDA; Single channel, He-Ne, Dantec Electronics, Mahwah, NJ) and ultrasonic triple crystal transducer measurements were made at radial positions of 0.75 mm, 1.1 mm, and 1.45 mm (design radial position + vessel wall thickness) away from the wall. Both the PUDV and LDA measurements were compared to the theoretically predicted velocities of steady fully developed (Poiseuille) flow. Wall shear rates were then computed from each set of three free stream velocity points together with the no slip assumption at the wall using a second-order curve fit.

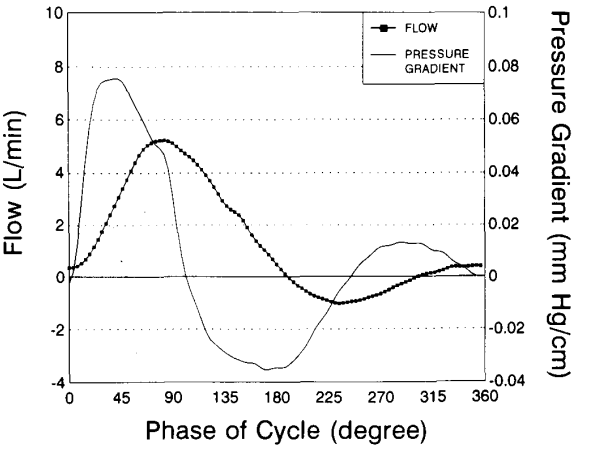

Fig. 3. Typical pressure gradient and flow waveforms generated by the pulsatile flow system.

Subsequently, the submersible pump was disconnected from the outflow of the reserve tank and the LVAD was enabled. An iliac artery waveform (Fig. 3) was simulated by operating the LVAD at a frequency of 0.25 Hz, which provided a Womersley parameter α = 3.5, $\mathrm{Re}_{\mathrm{mean}}$ = 200 and $\mathrm{Re}_{\mathrm{peak}}$ = 1000. Since the digital oscilloscope used in this experiment had only four channels, the pressure and flow waveforms for four cycles were first collected and then the PUDV velocity data was collected for four cycles. This procedure was repeated for a total of three runs. To eliminate high-frequency noise from the signal, each velocity waveform underwent discrete Fourier transform analysis, low-pass digital filtering (F_c = 3.75 Hz, or 15 Harmonics), and waveform reconstruction. In addition, low-pass filtering was performed on the digitized velocity data by implementing a moving weighted average with nine data points. In order to increase the accuracy of the shear rate data, each velocity waveform was corrected using the respective regression equations from the velocities obtained under pulsatile flow conditions. Shear rates were computed from the three PUDV velocity data points (plus wall no slip assumption) using second- and third-order curve fitting procedures. The pressure waveform and mean flow rate together with geometrical information and operating conditions were inputted into a Womersley computational model and compared to the velocities and shear rates measured with the ultrasonic triple crystal transducers.

III. Results

A total of 14 shear rate measuring transducers were fabricated (Fig. 4). Three of these did not survive the entire fabri-

Fig. 4. Three 20-MHz crystals imbedded in elastomer (actual transducer).

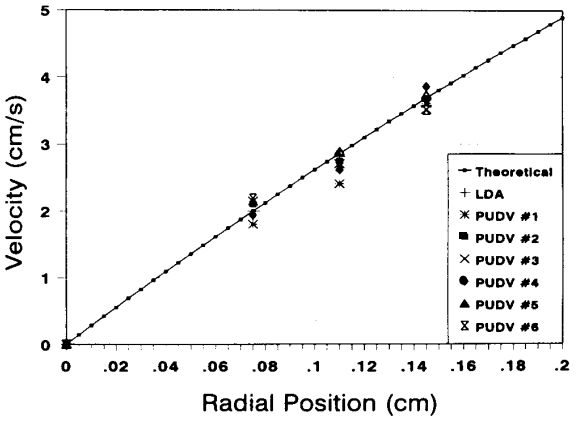

Fig. 5. Comparison of LDA, PUDV, and theoretical velocities for the same radial positions.

cation procedure due to wire or crystal breakage; therefore, 11 transducers were tested for compliance with design specifications using the direct dimensional validation technique. Optical measurements showed that individual intercrystal spacings were within 1.5 ± 1.0% error (maximum = ± 0.22 mm) compared to design. Furthermore, all crystals were placed within 2.0 ± 1.3% error (maximum = ± 8°) of the desired angle in each case.

A. Flow Validation

Five transducers failed during the *in vitro* testing due to corrosion and wire breakage. Thus, complete results for the remaining six transducers will be presented. For steady flow conditions, velocities measured by each PUDV crystal operating within its designed radial range compared well with corresponding LDA measurements (Fig. 5) having mean velocity percent errors of −2.0 ± 7.1% and differing by no more than 17% (0.5 cm/s) error. Furthermore, both PUDV and LDA techniques were within 16% (−1.8 ± 6.7%) and 7.5% (1.3 ± 3.2%) of the theoretically predicted velocities, respectively. The PUDV was found to generally underestimate, whereas the LDA generally overestimated the theoretical values. The absolute value of the percent errors of the velocity was found to be 5.7 ± 3.8% and 2.4 ± 2.4%, respectively. The shear rates computed from the triple crystal PUDV had a mean percent error of −4.3 ± 17.3% but no greater than 30%, and the corresponding LDA shear rates had a 5.9 ± 9.6% error with no greater than a 17.5% error from the theoretically predicted values. The absolute value of the shear rate mean percent errors were 12.7 ± 11.2% and 8.9 ± 6.2%, respectively. To evaluate repeatability of the measuring devices, three runs were performed on each device and the velocities were found to have a standard deviation of no greater than ± 0.11 cm/s from the mean.

Under pulsatile flow conditions, the velocities measured by each PUDV crystal operating at its designed radial range strongly correlated with the Womersley computational model with the cross-correlation coefficients ranging from 0.995–0.998, 0.996–0.999, and 0.995–0.999, respectively ($p <$ 0.01). The PUDV velocity waveforms had a phase lead of 3.6° relative to the Womersley velocity waveforms while having a similar shape. Typical Womersley velocity waveforms aligned in phase with the respective PUDV velocity waveforms are shown in Fig. 6. Overall, the PUDV velocities compared well with theoretically predicted velocities as evidenced by the range of the slopes and intercepts from the regression equations (Table I). In general, the mean, peak, and oscillatory (max-min) velocity percent errors were found to be within 20% of the theoretically predicted velocities. However, the 45° angle crystal was found to have the largest mean, peak, and oscillatory percent errors (Table II), primarily due to transducer number five which generated as much as a 39% error for these velocity intervals. Removal of this crystal from the error analysis improves the mean percent errors for the mean, peak, and oscillatory velocities to 0.315%, −6.938%, and −6.983%, respectively, with the standard deviations lying in the same range as the other crystals. Thus, this transducer was eliminated from any further analysis.

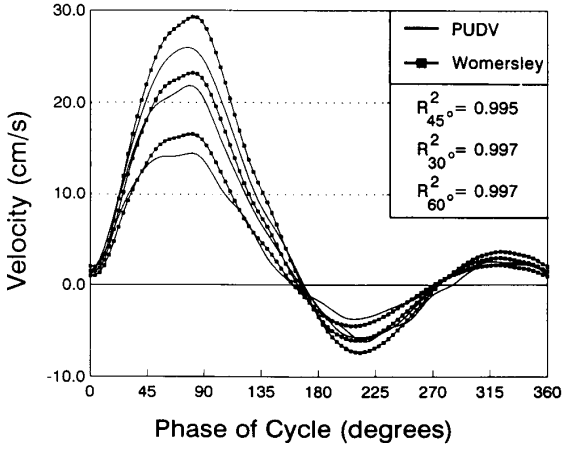

Fig. 6. Typical PUDV and Womersley velocity waveforms for one cardiac cycle at desired radial positions (transducer #6).

A product-moment correlation was conducted between the shear rates computed from the Womersley model and those

TABLE I
VELOCITY REGRESSION EQUATIONS AT DESIRED RADIAL POSITIONS FOR ALL TRANSDUCERS

	$V_D = mV_W + b$		
Tr. #	45° Crystal	30° Crystal	60° Crystal
1	$0.917V_W - 0.005$	$0.970V_W + 0.011$	$1.062V_W - 0.202$
2	$0.996V_W + 0.125$	$1.059V_W + 0.173$	$1.016V_W + 0.587$
3	$1.130V_W + 0.322$	$1.085V_W + 0.277$	$1.001V_W + 0.334$
4	$0.807V_W + 0.201$	$0.884V_W + 0.021$	$0.831V_W - 0.339$
5	$0.612V_W + 0.339$	$1.128V_W + 0.161$	$1.042V_W + 0.111$
6	$0.886V_W + 0.334$	$0.942V_W + 0.033$	$0.884V_W + 0.004$

TABLE II
SUMMARY OF THE VELOCITY PERCENT ERRORS FOR ALL TRANSDUCERS

		Mean ± SD		
	n	45° Crystal	30° Crystal	60° Crystal
Mean	6	-4.684 ± 17.700	3.442 ± 11.337	-1.299 ± 12.638
Peak	6	-12.292 ± 16.881	0.051 ± 9.109	-3.822 ± 9.815
Oscillatory	6	-12.199 ± 16.234	-0.403 ± 8.279	-4.509 ± 9.217

derived from the PUDV velocities using both second- and third-order curve fitting procedures. In general, the second-order curve fit appeared to better predict the Womersley shear rates since the correlation coefficients ranged from 0.981–0.996, compared to the third-order curve fit whose coefficients ranged from 0.923–0.986. Fig. 7 is a typical plot (transducer #6) of the shear rate regressions which illustrates the differences between the second- and third-order curve fitting results. Furthermore, the shear rate regression equations (Table III) show a very close similarity between the second- and third-order curve fits. Overall, the percent errors of the mean shear rates compared to the theoretical values were found to be within ± 1% for both the second- and third-order curve fits. It was noticed that the shear rates computed by the third-order curve fit were generally out of phase with the Womersley computed values, whereas the second-order computed shear rates were in phase. This phase irregularity can affect how the shear rate data is interpreted. For example, the second- and third-order peak shear rates were found to be within ± 10% and ± 22%, respectively, of the Womersley peak shear rates at the same time period. However, the absolute peak shear rates were found to be within ± 9% for both curve fits. Similarly, the oscillatory shear rates measured in phase with the theoretical values were within ± 13% and ± 25% for the second- and third-order fits, respectively, whereas absolute oscillatory shear rates were within ± 11% and ± 10% for the

TABLE III
SHEAR RATE REGRESSION EQUATIONS FOR ALL TRANSDUCERS

	$SR_D = mSR_W + b$	
Tr. #	2 nd Order	3 rd Order
1	$0.962SR_W + 1.762$	$1.004SR_W - 0.096$
2	$0.977SR_W + 1.148$	$1.022SR_W - 0.712$
3	$0.976SR_W + 1.124$	$0.969SR_W + 1.608$
4	$0.987SR_W + 0.436$	$0.967SR_W + 1.285$
6	$0.984SR_W + 0.621$	$0.954SR_W + 2.627$

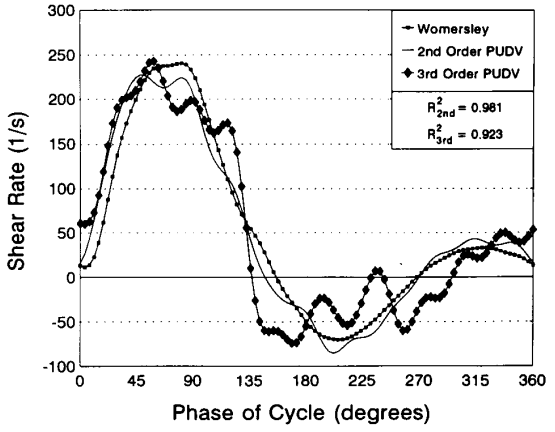

Fig. 7. Typical PUDV (second- and third-order) and Womersley shear rate waveforms (transducer #6).

TABLE IV
SUMMARY OF THE SHEAR RATE PERCENT ERRORS FOR ALL TRANSDUCERS

		Mean ± SD	
	n	2 nd Order	3 rd Order
Mean	5	-0.137 ± 0.276	0.210 ± 0.609
Peak	5	-5.548 ± 2.164	0.505 ± 5.683
Oscillatory	5	-2.443 ± 5.711	4.108 ± 5.702

second- and third-order fits, respectively. Table IV summarizes the average percent errors of the absolute shear rates for all transducers.

IV. DISCUSSION

With increased evidence of potential interaction between near-wall hemodynamics and vascular pathology [24], it has become necessary to develop means by which accurate, high-

resolution fluid dynamic measurements can be obtained *in vivo*. Results from the present study demonstrate the feasibility of fabricating a novel triple-crystal ultrasonic Doppler transducer which is capable of accurately measuring wall shear rates. This shear rate measuring device features a number of important capabilities for use under *in vivo* conditions, including: nonintrusiveness, high spatial resolution, and ability to obtain bidirectional velocities at multiple radial locations. Furthermore, the resolution of this device is sufficient to measure velocities within the boundary layer of many mid- to large-size vessels. This feature is important since it is within the boundary layer where velocity gradients and, thus, shear rates are developed. Due to its small size and weight, the transducer may also be positioned at various sites along the vessel wall to provide multiple shear rate measurements. The device may also be sterilized using gas sterilization techniques for measurements in chronic experiments.

There are several advantages to this ultrasonic transducer over existing wall shear rate measuring techniques. Although the LDA performs better under *in vitro* conditions, it is excluded from *in vivo* applications because of its requirement for a transparent medium. Other techniques that have been utilized for *in vivo* measurement of shear rate include: electromagnetic flowmeter (EMF) [8], hot film anemometry [6], and single-crystal PUDV [17], [18], [20], [21] methods. The EMF derived technique consists of using the mean flow rate together with the Poiseuille flow assumption to estimate the wall shear rates. One underlying assumption of Poiseuille flow is that the flow is steady which neglects the pulsatility of flow *in vivo*. Furthermore, this technique is unable to determine shear rates at multiple axial locations. Major limitations of hot-film anemometry are that it is invasive to the flow field and it is not easily repositioned to other axial locations. It is also limited in that it cannot distinguish flow direction such as exists in recirculation and stagnation regions. Finally, the single-channel pulse Doppler has the limitation of not being capable of obtaining velocity measurements along a line perpendicular to the vessel wall, but only along a line at an angle to the wall. Thus, shear rates calculated from this data are not true shear rates at particular axial sites, especially when used in regions where flow is not fully developed. Recent work in our laboratory [19] has shown that increasing the number of velocity points measured near the vessel wall improves the accuracy of the wall shear rate measurement. Therefore, shear rates derived from single-point velocity measurements using a single-crystal PUDV would have less accuracy than those obtained with the multicrystal PUDV presented in this study. Another advantage of this triple-crystal transducer is its ability to collect all velocity data simultaneously, as compared to other techniques which obtain velocity information sequentially.

Although this new ultrasonic device is an improvement over existing techniques, it is not without its limitations. Even though the maximum linear range of operation for this system is 10 mm, the system should be operated within the ultrasonic near field of each crystal to avoid significant signal attenuation and loss of lateral resolution. Since the narrowest part of the beam for each crystal is approximately 3 mm, the maximum radial depths that can be attained are 1.50, 2.12, and 2.60 mm for crystals at beam angles of 30°, 45°, and 60°, respectively. A second limitation of this device is its fragility and limited durability as demonstrated by the number of transducers which failed (8 of 14) during this study. In the future, modifications should be made to increase the longevity of this device, i.e., embedding crystals in a tougher material, avoiding contact of wires with corrosives, etc.

There are several factors which may account for the variances in velocities obtained experimentally. Under steady flow conditions, some particle settling occurred which resulted in signal loss due to a decrease in the concentration of particles in solution. Under pulsatile flow conditions, however, particle settling was not a problem since pulsatile motion of the fluid maintained the particles in suspension. Despite the care taken in maintaining proper alignment of individual crystals in each transducer, variability in alignment still existed with some crystals, appearing to be slightly rotated out of the plane of symmetry. In addition, some of the observed errors could be due to improper alignment of the transducer during the flush mounting procedure. Regarding the discrepancies which existed between velocities obtained from the spectrum analyzer and the ZCC, these were greater at lower frequencies and may be due to the cut-off levels of the high-pass filters in each device. Since the spectrum analyzer had a lower cut-off frequency (F_c = 80 Hz) than the ZCC (F_c = 160 Hz), it would more accurately detect the lower mean velocities which were generally present in the recordings.

The PUDV and LDA experimental measurements tended to either uniformly underestimate or overestimate the theoretically predicted velocities. These differences may be due to the Womersley model predicting velocities at a single infinitesimally small point whereas the experimental devices detected velocities within a finite sample volume. They may also be due to the shape of the velocity profile since more spectral broadening is produced as the velocity gradient increases. Sample volume size may account for the discrepancies of the velocity values obtained in comparing the ultrasonic device to the LDA since the length of the PUDV sample volume (0.31 mm) is larger ($\sim$ 50%) than that of the LDA (0.2 mm), and thus, more spectral broadening will occur with the ultrasonic device and result in lower average velocities. In addition, slower moving particles will have longer residence times when passing through the larger measuring volume and contribute more to the velocity calculation. Regarding differences between recordings for each crystal, the greatest amount of spectral broadening generally occurred with the 45° beam angle crystal (effective radial depth = 0.35 mm), which suggests that the location of the sample volume within the velocity profile has a greater effect on spectral broadening than does the beam angle. Otherwise, the 60° beam angle crystal would be expected to display the greatest amount of spectral broadening because of its greater radial sample volume length.

Finally, the mean shear rates obtained using either a second- or third-order curve fit were extremely accurate and exceeded expectations. While the in phase peak and oscillatory shear rates were inaccurate by up to 22% when computed with a third-order curve fit, these errors were possibly due to

misaligning the transducer between the pressure ports used in the theoretical calculation. This should not be a practical limitation, however, since only the absolute peak and oscillatory shear rates would typically be obtained and both curve fit procedures did provide accurate results for these parameters. The larger fluctuations seen with the shear rate waveforms using a third-order fit may be due to its greater sensitivity to changes in the near wall velocity measurement (0.35 mm) which are more pronounced at lower velocities.

The device presented in this paper will be a useful tool in obtaining hemodynamic information from a variety of normal and pathological models *in vivo*, e.g., atherosclerotic lesions, bypass graft hyperplasia, and vascular remodeling. This device also has the capability of obtaining 2-D velocity components, with no loss in performance, by simply rotating the transducer 180° and obtaining velocity measurements along a symmetrical axis. This would be valuable in nonaxial flow situations, e.g., vortices, separation and stagnation regions, etc. Furthermore, transducer fixtures and gantries can be constructed to enable this device to move freely with the arterial vessel wall and to repeatably obtain velocity measurements at multiple axial locations. Since it has been shown that shear *stresses* and not shear *rates* elicit biological responses [25], the information obtained from this device can be used to estimate shear stresses for both Newtonian and non-Newtonian fluid behavior. For Newtonian behavior, as seen in large arterial vessels, shear forces can be obtained by multiplying the shear rate by the dynamic viscosity of whole blood. Similarly, shear stresses can also be determined for non-Newtonian flow utilizing the shear values obtained from this device together with the shear rate dependent viscosity equations. In conclusion, this new triple-crystal PUDV transducer has been shown to be a viable device for measuring shear rate and is a technique which is superior to conventional methods.

ACKNOWLEDGMENT

The authors wish to acknowledge the technical support of G. Juengel, Machinist, College of Engineering Machine Shop. In addition, they would like to thank M. Nair, Graduate Student, Department of Biomedical Engineering and M. Evancho, Research Associate, Summa Health System Vascular Surgery Research Laboratory for technical assistance on this project. Furthermore, the authors wish to thank D. Medvick and The Swagelok Quick-Connect Company for use of their equipment.

REFERENCES

[1] R. M. Nerem and J. F. Cornhill, "The role of fluid mechanics in atherogenesis," *J. Biomechan. Eng.*, vol. 102, pp. 181–189, Aug. 1980.
[2] C. K. Zarins *et al.*, "Carotid bifurcation atherosclerosis: Quantitative correlation of plaque localization with flow velocity profiles and wall shear stress," *Circ. Res.*, vol. 53, no. 4, pp. 502–514, Oct. 1983.
[3] M. H. Friedman, O. J. Deters, and F. F. Mark, "Arterial geometry affects hemodynamics: A potential risk factor for atherosclerosis," *Atherosclerosis*, vol. 46, pp. 225–231, 1983.
[4] H. N. Sabbah *et al.*, "Relation of atherosclerosis to arterial wall shear in the left anterior descending coronary artery of man," *Amer. Heart J.*, vol. 112, no. 3, pp. 453–458, 1986.
[5] S. A. Bareli *et al.*, "Hemodynamics and low density lipoprotein metabolism: Rates of low density lipoprotein incorporation and degradation along medial and lateral walls of the rabbit aorto-iliac bifurcation," *Arteriosclerosis*, vol. 10, pp. 688–694, Sept./Oct. 1990.
[6] S. E. Rittgers *et al.*, "Velocity distribution and intimal proliferation in autologous vein grafts in dogs," *Circ. Res.*, vol. 42, pp. 792–801, 1978.
[7] H. S. Bassiouny *et al.*, "Quantitative inverse correlation of wall shear stress with experimental intimal thickening," *Surgical Forum: Congr. Amer. Coll. Surg.*, pp. 328–329, Oct. 1988.
[8] R. L. Binns *et al.*, "Optimal graft diameter: Effect of wall shear stress on vascular healing," *J. Vasc. Surg.*, vol. 10, pp. 326–327, 1989.
[9] P. B. Dobrin, F. N. Littooy, and E. D. Endean, "Mechanical factors predisposing to intimal hyperplasia and medial thickening in autogenous vein grafts," *Surg.*, pp. 393–400, Mar. 1989.
[10] V. S. Sottiurai *et al.*, "Distal anastomotic intimal hyperplasia: Histopathologic character and biogenesis," *Ann. Vasc. Surg.*, vol. 3, no. 1, pp. 26–33, 1989.
[11] M. C. S. Shu and H. H. C. Hwang, "Haemodynamics of angioaccess venous anastomoses," *J. Biomechan. Eng.*, vol. 13, pp. 103–112, Mar. 1991.
[12] R. J. Lutz, J. N. Cannon, K. B. Bischoff, R. L. Dedrick, R. K. Stiles, and D. L. Fry, "Wall shear stress distribution in a model canine artery during steady flow," *Circ. Res.*, vol. 41, pp. 391–399, 1977.
[13] P. Zhao-Hong, X. Bao-Shu, and N. H. C. Hwang, "Wall shear stress distribution in a model human aortic arch: Assessment by an electrochemical technique," *J. Biomechan.*, vol. 18, pp. 645–656, 1985.
[14] A. Kamiya, J. Ando, and M. Shibata, "Roles of fluid shear stress in physiological regulation of vascular structure and function," *Biorheology*, vol. 25, pp. 271–278, 1988.
[15] K. Inokuchi *et al.*, "A desktop computer to visualize the intraluminal velocity profile and its clinical application," *J. Vasc. Surg.*, vol. 1, pp. 787–794, 1984.
[16] K. Morinaga *et al.*, "Effect of wall shear stress on intimal thickening of arterially transplanted autogenous veins in dogs," *J. Vasc. Surg.*, vol. 2, pp. 430–433, 1985.
[17] M. K. Wells *et al.*, "Blood velocity patterns in coronary arteries," *J. Biomechan. Eng.*, pp. 26–31, Feb. 1978.
[18] D. R. Bell, H. N. Sabbah, and P. D. Stein, "Profiles of velocity in coronary arteries of dog indicate lower shear rate along inner arterial curvature," *Arteriosclerosis*, vol. 9, pp. 167–175, Mar./Apr. 1989.
[19] R. S. Fatemi and S. E. Rittgers, "Derivation of shear rates from near-wall LDA measurements under steady and pulsatile flow conditions," *J. Biomechan. Eng.*, vol. 116, pp. 361–368, Aug. 1994.
[20] A. P. G. Hoeks, R. S. Reneman, and P. A. Peronneau, "A multigate pulsed Doppler system with serial data processing," *IEEE Trans. Sonics Ultrason.*, vol. SU-28, pp. 242–247, 1981.
[21] S. A. Altobelli and R. M. Nerem, "An experimental study of coronary artery fluid mechanics," *J. Biomed. Eng.*, vol. 107, pp. 16–23, 1985.
[22] C. G. Caro, T. J. Pedley, R. C. Schroter, and W. A. Seed, *The Mechanics of the Circulation*. New York: Oxford University Press, 1978.
[23] Q. Yu, "Blood-intimal shear rate distribution at distal anastomoses of aortoiliac bypass grafts in dogs," M.S. thesis, University of Akron, OH, 1991.
[24] T. Yamaguchi and Y. Yoshida, "An international symposium on the role of blood flow in atherogenesis," *Arteriosclerosis*, vol. 8, pp. 445–448, 1988.
[25] J. Ando *et al.*, "Wall shear stress rather than shear rate regulates cytoplasmic Ca^{++} responses to flow in vascular endothelial cells," *Biochem. Biophys. Res. Commun.*, vol. 190, no. 3, pp. 716–723, Feb. 1993.

Robert S. Keynton received the B.S. degree in engineering science and mechanics from Virginia Polytechnic Institute and State University, Blacksburg, VA, in 1987, the M.S. degree in biomedical engineering from the University of Akron, Akron, OH, in 1990, and is currently completing the requirements for the Ph.D. degree in biomedical engineering at the University of Akron. His doctoral dissertation concerns the design, development, and implementation of a micro-ultrasonic shear rate measuring device for use in an *in vivo* model to determine the effect of vascular graft diameter mismatch upon wall shear rate and intimal hyperplasia.

His research interests have primarily focused on vascular hemodynamics and its affect on biological tissue.

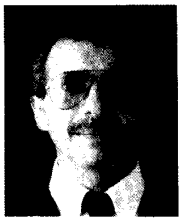

Richard E. Nemer was born in Akron, OH, in 1957. He received the B.S. degree in electronic engineering technology with a minor in instrumentation technology from the University of Akron in 1983.

From 1976 to 1978, he was employed by Radian Electronics of Akron, OH as an Electronics Designer and Special Project Coordinator. From 1979 to 1982, he worked for the Departments of Biology and Chemical Engineering at the University of Akron. Since 1983, he has been employed by the University of Akron's College of Engineering in the Department of Biomedical Engineering and the Institute for Biomedical Engineering Research.

Qianhui Y. Neifert was born in Jinan, The Peoples Republic of China in 1964 and received the B.S. degree from Shanghai Jiao Tong University in 1987. She received the M.S. degree in biomedical engineering from the University of Akron in 1991 and is currently pursuing her Ph.D. degree in biomedical engineering using a finite element model of the breast for application to cancer detection.

Ray S. Fatemi received the B.S. degree in biomedical engineering in 1983, the M.S. in 1985, and the Ph.D. in 1990 in mechanical engineering from the University of Iowa.

In 1990, he joined the Biomedical Engineering program at the University of Akron as a Research Assistant Professor where he has engaged in vascular dynamics research. He is currently President of Accu-Tek of Ohio, Inc., Akron, OH, a biomedical research, product development, manufacturing, and marketing company. In addition, he is currently an Adjunct Faculty Member of the Department of Biomedical Engineering at the University of Akron.

Stanley E. Rittgers received the B.S. degree in mechanical engineering from the State University of New York at Buffalo in 1968, the M.S. in mechanical engineering in 1975, and the Ph.D. in biomedical engineering in 1978 from the Ohio State University, Columbus, OH.

From 1978 to 1984 he was a Research Scientist at the Veterans Administration Hospital and an Assistant Professor in the Biomedical Engineering Program at Virginia Commonwealth University in Richmond, VA. He became an Associate Professor of Biomedical Engineering at the University of Akron in 1984 and Professor of Biomedical Engineering in 1992. He also holds the position of Director, Institute for Biomedical Engineering Research at the University of Akron. His interests involve noninvasive vascular diagnosis, cardiovascular modeling, and arterial graft patency.